Excited-state dynamics of alizarin-sensitized TiO_2 nanoparticles from resonance Raman spectroscopy

Lian C. T. Shoute, and Glen R. Loppnow

Citation: The Journal of Chemical Physics **117**, 842 (2002); doi: 10.1063/1.1483848
View online: https://doi.org/10.1063/1.1483848
View Table of Contents: http://aip.scitation.org/toc/jcp/117/2
Published by the American Institute of Physics

Excited-state dynamics of alizarin-sensitized TiO_2 nanoparticles from resonance Raman spectroscopy

Lian C. T. Shoute and Glen R. Loppnow[a)]
Department of Chemistry, University of Alberta, Edmonton, Alberta, Canada

(Received 15 February 2002; accepted 15 April 2002)

Resonance Raman spectra of alizarin-sensitized TiO_2 nanoparticles have been obtained at excitation wavelengths throughout the 488-nm charge transfer absorption band. The resonance Raman spectrum of the alizarin-sensitized TiO_2 nanoparticle is significantl different from the spectrum of free alizarin, consistent with a chemisorption-type interaction. This interaction is probably chelation of surface titanium ions by the hydroxy groups of alizarin, supported by the observed enhancement of bridging C–O modes at 1326 cm^{-1}. In contrast to resonance Raman intensity analysis of homogeneous electron transfer where vibrations of both the donor and acceptor are observed, self-consistent analysis of the resulting resonance Raman excitation profile and absorption spectrum using the time-dependent wave packet propagation formalism show mode-specifi reorganization along alizarin vibrations exclusively; no resonance-enhanced vibrations attributable to the TiO_2 moiety are observed. Therefore, the total resonance Raman-derived reorganization energy is only 0.04 eV, significantl smaller than the observed outer-sphere reorganization energy of 0.2 eV for this system and inner-sphere reorganization energies measured for other molecular systems. The discrepancy is ascribed to a significan environmental component to the outer-sphere reorganization energy arising from rapid dephasing of surface TiO_2 units involved in adsorption by strongly coupled interior bath vibrations. © *2002 American Institute of Physics.*
[DOI: 10.1063/1.1483848]

I. INTRODUCTION

The dynamics of interfacial electron transfer from discrete energy states of dyes to the conduction band manifold of the semiconductor nanoparticle to which they have been adsorbed has been intensively investigated in recent years.[1–5] The motivation for these investigations has been to better understand the factors affecting interfacial electron transfer in processes such as electrochemistry and photography,[6] and the desire to design and build more efficien solar photovoltaic cells.[7–10] Recent advances in preparing transparent nanoparticles have enabled researchers to probe these processes with optical techniques such as absorption and fluorescenc spectroscopies with femtosecond time resolution.[11–13] Charge injection processes in a wide variety of dye sensitized TiO_2 nanoparticles have been reported to follow multicomponent kinetics.[14–17] The kinetics of electron injection from excited fluorescei 27 to TiO_2 is characterized by three time constants <0.1, 0.9, and 8 ps.[16] For $Ru(dcpby)_2(NCS)_2$ (dcbpy=2,2′-bipyridyl-4,4′-dicarboxylate) sensitized TiO_2 nanoparticles, the major component of the charge injection takes place in 50 fs and the minor process has a lifetime of 1.7 ps.[18] Ultrafast electron transfer from excited dye to the conduction band of TiO_2 nanoparticles has been reported for dyes such as coumarin-343,[19] porphyrins,[20] phthalocyanines,[21] xanthene,[16] squarine,[22] and anthracene[23] dyes.

A common feature of dye-sensitized TiO_2 systems exhibiting ultrafast electron injection is that the dye is covalently linked to the TiO_2 by one or more ester groups formed by reaction between the dye carboxylic substituent and the surface hydroxyl group on the TiO_2.[24,25] The formation of a covalent bond bridge increases the interaction between the π^* orbital of the dye and the $3d^0$ orbital of Ti^{4+}, enhancing the electron coupling. It is possible that the electronic coupling is strong enough in these systems to put electron transfer reaction in the adiabatic regime. The dramatic decrease in the injection rate[14,26] observed on introducing a bridging $-CH_2-$ between the anchoring carboxylic group and the dye in Re-bipyridyl complexes, $Re(CO)_3Cl[dc(CH_2)_n bpy]$, adsorbed to TiO_2 is evidence that electronic coupling perhaps plays a decisive role in these processes.

The rate of electron transfer in the nonadiabatic limit is generally described by a Golden Rule expression,[27]

$$k=(2\pi/h)|V|^2(\mathrm{FCWD}). \tag{1}$$

The donor–acceptor electronic coupling element V contains the dependence of the rate on orientation of the reactants and their separation distance. The Franck–Condon factors, FCWD, contain the dependence of the rate on density of states and the total reorganization energy. For electron transfer between molecules in solution, FCWD includes contributions from solvent motions and contributions from all the vibrational modes of the donor and the acceptor coupled to the electron transfer. Therefore, in order to properly account for factors affecting electron transfer, the frequencies and reorganization energies of these individual internal modes must be known.

a)Author to whom correspondence should be addressed. Electronic mail: glen.loppnow@ualberta.ca

Resonance Raman spectroscopy is an ideal probe of mode-specifi reorganization energies resulting from charge transfer transitions.[28–32] The resonance Raman frequencies reflec the geometry of the ground state, while the intensities reveal the excited state geometry change upon charge transfer.[28,30] Raman vibrational studies of surface adsorption and interfacial electron transfer have been reported by a number of groups. Early studies showed that the Raman and absorption spectra exhibit significan frequency (wavelength) shifts and intensity (absorbance) changes as a result of strong bonding between the surface species and adsorbate upon chemisorption,[33–36] with much smaller frequency and intensity observed changes for physisorption.[37–39] More recently, resonance Raman spectroscopy has been used to determine reorganization energies for charge transfer in dye-sensitized TiO_2.[40]

In this paper, we report the resonance Raman spectra and resulting analysis of a heterogeneous electron transfer system, alizarin adsorbed on TiO_2 nanoparticles. Alizarin forms a strong charge transfer complex upon adsorption to a TiO_2 nanoparticle[41] and exhibits an intense charge transfer absorption band at 488 nm, shifted to lower energies by 2800 cm^{-1} from the free alizarin absorption band. Excitation into this band is known to lead to electron injection from the excited alizarin to the conduction band of TiO_2 within 100 fs.[41] Ultrafast electron injection quenches the fluorescenc originating from excited state alizarin. Hence, alizarin adsorbed on TiO_2 forms an ideal heterogeneous charge transfer system to study using resonance Raman spectroscopy. The resonance Raman spectrum of the charge transfer complex is signifi cantly different from the free dye in solution, arguing for a chemisorption-type interaction, probably via chelation of surface titanium ions by the hydroxy groups of alizarin. The absolute Raman cross sections and resulting mode-specifi reorganization energies of the alizarin–TiO_2 complex measured here indicate that the major component of the reorganization energy arises from the nanoparticle itself, as a result of rapid dephasing into the interior from surface states after electron injection.

II. EXPERIMENT

Colloidal nanoparticles of TiO_2 were prepared from $TiCl_4$ (Aldrich, Milwaukee, WI) by a procedure described in the literature.[41,42] Briefl , 1.5 ml of titanium tetrachloride (Aldrich, Milwaukee, WI) prechilled to <0 °C was added slowly to 100 ml of vigorously stirred deionized water at <1 °C. After continuous stirring for 30 min at this temperature, the reaction mixture was dialyzed (MW cutoff 3500) for 7–8 h at room temperature using 5–6 l of deionized water to bring the *p*H of the solution to about 3. No polymer was added in the solution to stabilize the colloids. With this procedure, the average diameter of the TiO_2 particles should be ~16 nm, based on earlier studies.[41] The alizarin–TiO_2 nanoparticle charge transfer complex was prepared by slowly adding alizarin (Aldrich, Milwaukee, WI) into vigorously stirred colloidal TiO_2 in water. The complex has a molar absorption coefficien of 8690 $M^{-1}\,cm^{-1}$ at the absorption maximum at 486 nm.

The experimental setup for measuring resonance Raman spectra and depolarization ratios was described earlier.[43] Laser excitation lines to cover the entire charge transfer band of the alizarin–TiO_2 complex were obtained from a Coherent Ar ion cw laser (457.9, 488, and 514.5 nm) and a Coherent Kr ion cw laser (406.7, 530.9, and 647.1 nm). The excitation laser beam was tightly focused onto a spinning 5 mm o.d. NMR tube containing the sample. The scattered Raman signals were collected in a 135° backscattering geometry and coupled into a spectrometer as described previously.[43] Samples for resonance Raman spectrum measurements contain ~1 mM alizarin complexed to TiO_2 nanoparticles, as determined from absorption spectroscopy by using a diode array spectrophotometer (Hewlett–Packard, Model 8452A), and 2.1 M dimethyl sulfoxide (ACP Chemicals, Inc.). Dimethyl sulfoxide (DMSO) was added as the internal standard for absolute Raman cross section determination and had no effect on the measured absorption and resonance Raman spectra. Measurement of the resonance Raman spectra and determination of the intensities were repeated on 3–4 fresh samples of the alizarin–TiO_2 complex containing 2.1 M DMSO. The sample spectra were frequency calibrated with known solvent Raman peaks and intensity corrected for the spectrometer detection efficienc by using a standard lamp spectrum (Electro-Optics Associate) and standard lamp output. Data analysis and the method followed to determine absolute Raman cross sections from the experimentally measured resonance Raman intensities have been described previously.[43,44]

The absolute Raman cross sections of DMSO in aqueous solution at *p*H 3 were determined separately using the 1047 cm^{-1} Raman line of NO_3^- as a standard.[44] Raman spectra of 2.1 M DMSO aqueous solution containing 0.5 M NO_3^- (*p*H 3) were measured for laser excitation wavelengths at 406.7, 457.9, 488, 514.5, 530.5, and 647.1 nm. No difference was seen in the absolute cross section of nitrate between *p*H 7 and *p*H 3. The Raman cross sections for DMSO at each excitation wavelength were calculated from the relative Raman intensities and concentrations as described previously.[43,44] An A-term equation [Eq. (2)] was fi to the resulting DMSO Raman cross sections obtained for the 677 cm^{-1} band of DMSO,

$$\sigma_R = \frac{8\pi}{3}\left(\frac{1+2\rho}{1+\rho}\right) K \nu_0 \nu^3 \left[\frac{\nu_e^2+\nu_0^2}{(\nu_e^2-\nu_0^2)^2}+C\right]^2 \qquad (2)$$

to yield $K=9.16\times10^{-30}$ cm^2/molecule, $\nu_e=51\,940$ cm^{-1}, and $C=2.42\times10^{-9}$ cm^{-2}. Equation (2) with these parameters was then used to calculate the absolute Raman cross sections of DMSO at each excitation wavelength.

III. THEORY

The resonance Raman intensities were simulated with the time-dependent wave packet propagation formalism,[30,31]

$$\sigma_R = \frac{8\pi E_S^3 E_L e^4 M^4}{9\hbar^6 c^4} \int_{-\infty}^{\infty} dE_0 H(E_0) \left| \int_0^{\infty} dt \langle f | i(t) \rangle \times \exp\left\{ \frac{i(E_L + \epsilon_i)t}{\hbar} \right\} G(t) \right|^2, \quad (3)$$

$$\sigma_A = \frac{4\pi E_L e^2 M^2}{6\hbar^2 cn} \int_{-\infty}^{\infty} dE_0 H(E_0) \int_{-\infty}^{\infty} dt \langle i | i(t) \rangle \times \exp\left\{ \frac{i(E_L + \epsilon_i)t}{\hbar} \right\} G(t), \quad (4)$$

where E_L and E_S are the energies of the incident and scattered photons, respectively, n is the refractive index, M is the transition length, ϵ_i is the energy of the initial vibrational state, $|i\rangle$ and $|f\rangle$ are the initial and fina vibrational wave functions, $H(E_0)$ is a normalized inhomogeneous distribution of site electronic energies (usually assumed to be Gaussian), $G(t) = \exp(-4\pi^2\Gamma^2 t^2/h^2)$ is the homogeneous linewidth function, and $|i(t)\rangle = \exp(-i2\pi Ht/h)|i\rangle$ is the initial ground-state vibrational wave function propagated on the excited-state potential surface. The application of these equations to the resonance Raman intensities of charge transfer systems has been described in detail.[31,32]

For the analysis presented here, the initial guesses for the displacements along each normal coordinate (Δ) were found from the relative resonance Raman vibrational intensities at 458 nm assuming the intensities were proportional to Δ^2 and with the intensity of the 1462 cm^{-1} mode set arbitrarily to 1. All 20 observed fundamental vibrational modes were used in the time-dependent calculations. Other parameters were selected to give the best calculated absorption spectrum and resonance Raman excitation profiles The parameters were then optimized iteratively as described previously[30,31,43,44] until the calculated and experimental absorption spectrum and resonance Raman excitation profile were in agreement.

IV. RESULTS

Figure 1 shows the absorption spectra of free alizarin in aqueous solution, TiO_2 and the alizarin–TiO_2 (Alz|TiO_2) complex, all at *p*H 3. The emission spectrum of free alizarin is also shown. Upon bonding to a TiO_2 nanoparticle, the alizarin visible absorption band appears to undergo a 58 nm (2800 cm^{-1}) shift to lower energy. Shifts of absorption maxima are seen in other dye-sensitized semiconductor nanoparticles, although the direction and magnitude is highly system dependent. Studies have shown that the shifted absorption band in the Alz|TiO_2 complex is actually a new charge transfer absorption band.[41] Further evidence for the formation of the new charge transfer band are the quenching of the normally weak alizarin fluorescenc band centered at 635 nm upon binding to TiO_2, suggesting a new electronic character of the excited state, and the different resonance Raman spectrum observed with excitation into this new band compared to the dye alone (*vide infra*).

Figure 2 shows the resonance Raman spectra of the Alz|TiO_2 complex, free alizarin in DMSO solution, 2.1 M DMSO/H_2O solvent and 2×10^{-6} M of colloidal TiO_2 nanoparticles (0.14 M TiO_2) excited at 488 nm. Note that with excitation within the complex charge transfer band, no contributions to the resonance Raman spectrum of the complex come from either free alizarin [Fig. 2(b)] or uncomplexed TiO_2 [Fig. 2(d)]. The Alz|TiO_2 complex in DMSO/water spectrum exhibits 29 Raman bands, 20 of which are resonantly enhanced by the 488-nm excitation of the charge transfer band. Of the remaining bands in Fig. 2, those at 677, 713, 952, 1020, and 1418 cm^{-1} are Raman bands of DMSO in aqueous solution. The small feature near 740 cm^{-1} is a detector artifact. Weak vibrations at 841, 1572, and 1587 cm^{-1} were Alz|TiO_2 Raman bands resonantly enhanced by a higher lying state ~300 nm. No Alz|TiO_2 complex vibration bands were observed at frequencies below 600 cm^{-1} or above 1700 cm^{-1}; only vibrations from the DMSO/water solvent were observed below 600 cm^{-1}. No vibrational bands attributable to TiO_2 were observed in the resonance Raman spectra of the complex.

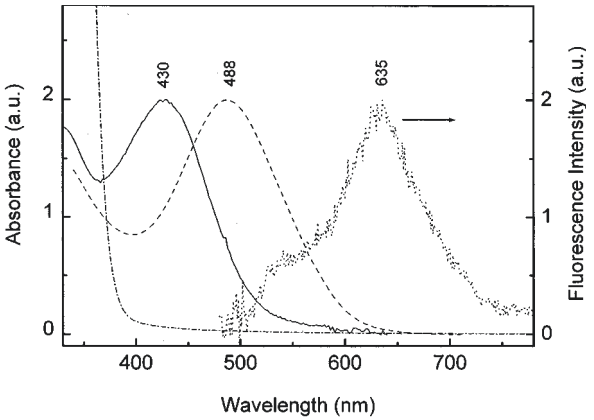

FIG. 1. Absorption spectra of alizarin (—), TiO_2 (–·–), and alizarin-–TiO_2 complex (---) in aqueous solution at *p*H 3. The spectrum of TiO_2 has been subtracted from the spectrum of the alizarin–TiO_2 complex. The fluores cence spectrum of free alizarin in aqueous solution at *p*H 3 is also shown (···).

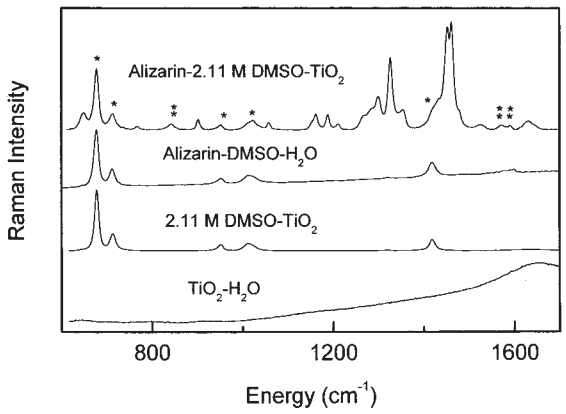

FIG. 2. 488 nm excited resonance Raman spectra of the Alz|TiO_2 complex, free alizarin, solvent, and colloidal TiO_2 nanoparticles in aqueous/DMSO solution at *p*H 3. In the spectrum of the Alz|TiO_2 complex, asterisks (*) indicate solvent peaks and double asterisks (**) indicate spectrometer artifacts or modes which are not resonantly enhanced by the 488 nm absorption band.

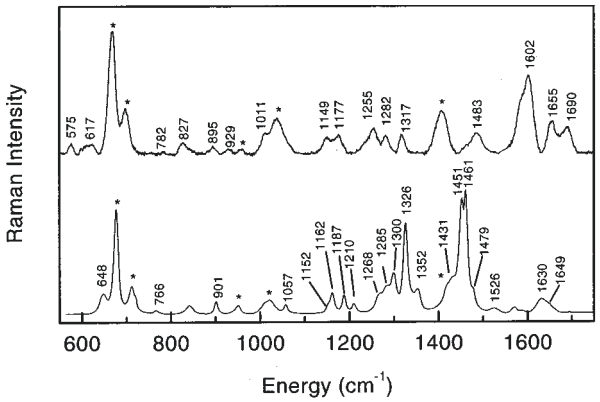

FIG. 3. 375 nm excited resonance Raman spectrum of 0.1 M free alizarin (a) and 488 nm excited resonance Raman spectrum of 10^{-3} M Alz|TiO_2 complex in aqueous solution at *p*H 3. All of the labeled peaks in the Alz|TiO_2 complex spectrum were used in the resonance Raman intensity analysis. Asterisks (*) indicate solvent peaks.

With excitation at 375 nm to avoid the natural fluorescenc background from the dye, the resonance Raman spectrum of 0.1 M alizarin in solution exhibits several weak peaks [Fig. 3(a)], compared to the spectrum of 10^{-3} M Alz|TiO_2 complex [Fig. 3(b)] with some contributions from the DMSO/H_2O solvent [Fig. 2(c)]. Excitation at 375 nm of the Alz|TiO_2 complex in solution yields a spectrum of solvent only. Table I lists the vibrational assignments of the 20 resonance-enhanced vibrational modes of the Alz|TiO_2 complex. These assignments are based on previous assignments of 9,10-anthraquinone,[45] 1,4-dihydroxy-9,10-anthraquinone,[46] and 1,8-dihydroxy-9,10-anthraquinone.[47] The strongest features in the resonance Raman spectrum of the Alz|TiO_2 complex are the ring stretches at 1451 and 1461 cm^{-1}, and the C–O stretch at 1326 cm^{-1}. Moderate intensity is observed for the carbonyl stretch at 1630 cm^{-1}, C–O stretches coupled with ring stretches at 1268–1300 cm^{-1}, and in-plane C–H and C–O deformation bands at 1152–1210 cm^{-1}. The band at 648 cm^{-1} in the Alz|TiO_2 complex is not observed in uncomplexed alizarin and may be due to a Ti–O stretch[48,49] from a bridging Ti–O–C bond; bands due to Ti–O stretching vibrations of peroxo- and alkoxide-type complexes[50,51] occur in the 500–657 cm^{-1} region and the anatase form of TiO_2 has a Ti–O stretching mode at 635 cm^{-1}. The mode frequencies and relative intensities of the uncomplexed alizarin spectrum in Fig. 3(a) are quite different from those of the Alz|TiO_2 complex in Fig. 3(b). The uncomplexed alizarin has the C═C ring stretch as the strongest band at 1602 cm^{-1}, and other moderately strong bands are due to the carbonyl stretch (1655 and 1690 cm^{-1}), C–O and ring stretch (1255–1317 cm^{-1}), and C–H and C–O deformations at 1149–1177 cm^{-1}. These differences between the free alizarin spectrum and the Alz|TiO_2 complex spectrum excited at wavelengths within the 488-nm absorption band suggest that the excited-state is different when alizarin adsorbs to TiO_2, consistent with the shifts observed in the absorption spectrum, and suggesting chemisorption of the alizarin to the TiO_2 nanoparticle, probably via the hydroxyl groups[24,25,41] and/or the carbonyl.[52]

Figure 4 shows the resonance Raman spectra of the Alz|TiO_2 complex as a function of excitation wavelength within the 488-nm charge transfer absorption band. The simi-

TABLE I. Resonance Raman parameters of the alizarin–TiO_2 charge transfer complex.[a]

ν (cm^{-1})	ρ (at 488 nm)	$\lvert\Delta\rvert$	λ_i (cm^{-1})	Assignment
648	0.42	0.24	18.7	skeletal+TiO_2 stretch
766	0.38	0.067	1.72	out-of-plane OH stretch+skeletal
901	0.43	0.116	6.06	skeletal
1057	0.39	0.097	4.97	in-plane CH bend
1152	0.38	0.062	2.21	in-plane CH bend
1161	0.38	0.138	11.1	in-plane CH bend
1187	0.39	0.125	9.27	in-plane CH bend
1210	0.46	0.091	4.96	in-plane OH bend
1268	0.33	0.157	15.6	C–O stretch+ring stretch
1285	0.50	0.162	16.9	ring stretch+C–O stretch
1300	0.37	0.158	16.2	C–O stretch+ring stretch
1326	0.39	0.316	66.2	C–O stretch+ring stretch
1352	0.39	0.131	11.6	ring stretch
1431	0.41	0.139	13.8	ring stretch
1451	0.39	0.292	61.9	ring stretch
1461	0.39	0.30	65.8	ring stretch
1479	0.37	0.059	2.60	ring stretch
1526	0.42	0.069	3.63	ring stretch
1630	0.36	0.12	11.3	C═O stretch
1650	0.53	0.086	6.06	C═O stretch
Total			351 (0.04 eV)	

[a]The parameters used in the fittin are zero–zero energy $E_{00}=20\,010$ cm^{-1}, Gaussian homogeneous broadening $\Gamma=573$ cm^{-1}, inhomogeneous broadening $\Theta=1620$ cm^{-1}, transition length $M=1.045$ Å. Errors in Δ are $\pm 40\%$ and are $\pm 10\%$ in the other parameters.

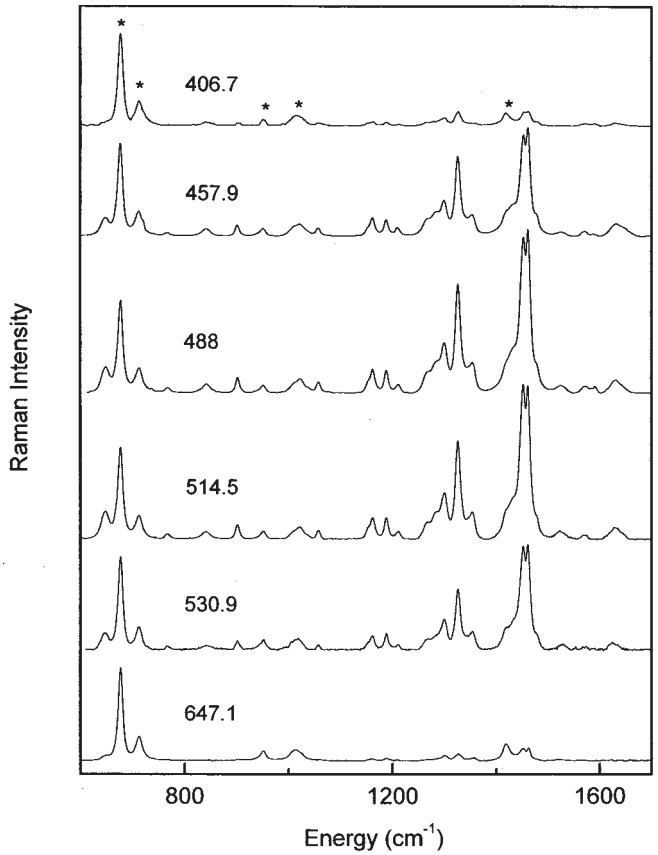

FIG. 4. Resonance Raman spectra of alizarin adsorbed on TiO_2 colloidal nanoparticles in aqueous solution at *p*H 3 as a function of excitation wavelength. Asterisks (*) indicate solvent peaks.

larity of the relative intensities as the excitation wavelength is tuned from 407 to 647 nm argue that this absorption band probably contains a single electronic transition which alone enhances the Raman vibrations. This conclusion is also supported by the fact that the depolarization ratio of all of the modes used in the resonance Raman analysis are 0.33 (Table I) within experimental error, the expected value for totally symmetric modes resonantly-enhanced by a single allowed electronic transition. No frequency shifts are observed in the spectra as a function of excitation wavelength, again consistent with a single electronic transition. The observed intensity decrease in all of the Alz$|TiO_2$ vibrational bands compared to the DMSO solvent bands as the excitation wavelength is tuned outside the charge transfer absorption band is a clear demonstration of the resonance enhancement effect and further suggests that the vibrational modes are resonantly enhanced by a single electronic state.

Figures 5 and 6 show the good agreement between the calculated and experimental absorption band and resonance Raman excitation profiles respectively, using the time-dependent formalism of resonance Raman spectroscopy [Eqs. (3) and (4)]. The experimental and calculated resonance Raman parameters are collected in Table I.[35] It must be noted that the absorption spectrum is diffuse and no overtone/combination band intensities were observable. In cases such as this, the Raman parameters may be somewhat ambiguous. Here, the reported deltas are accurate to ±40%,

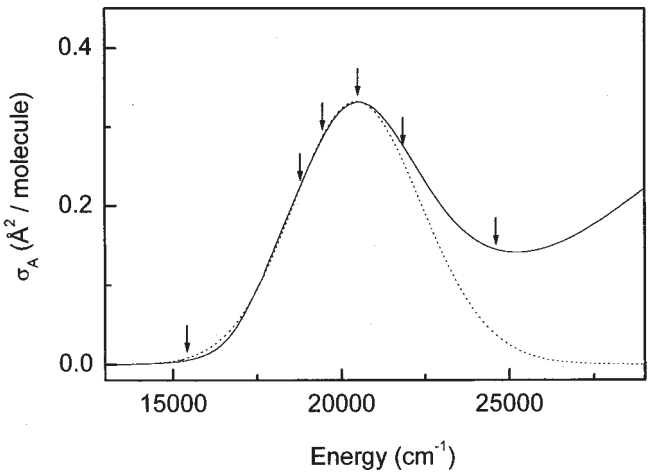

FIG. 5. Experimental (—) and calculated (––) absorption spectra of alizarin adsorbed on colloidal TiO_2 nanoparticles in aqueous solution at *p*H 3. Arrows indicate the resonance Raman excitation wavelengths used in this work.

with much smaller errors of ~10% in the other parameters, and are ultimately constrained by the magnitudes, bandwidths, and band shapes of the absorption spectrum and resonance Raman excitation profiles Although the error in the deltas is large, the conclusions given below are largely independent of the precise value of the deltas. Clearly, the simulations support the suggestion that the 488-nm absorption band contains a single electronic transition. The observed deviations between the calculated and experimental absorption spectrum at high energies come from higher-lying electronic transitions which contribute no resonance enhancement to the observed vibrations and are therefore not modeled by the simulations.

V. DISCUSSION

A. Mechanism of adsorption

Resonance Raman spectroscopy provides a spectral signature for adsorption. In this work, the resonance Raman and

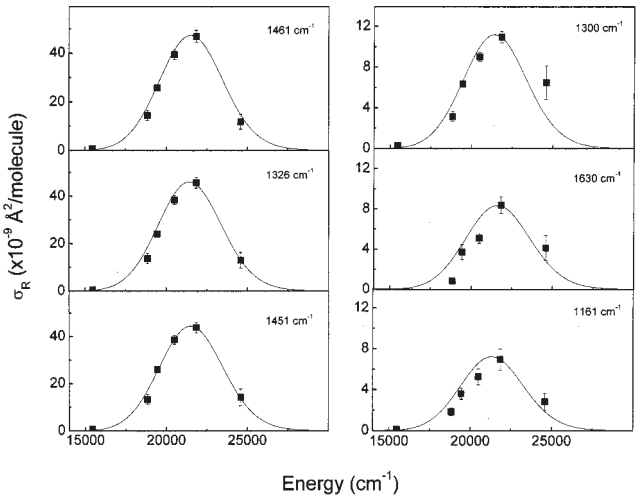

FIG. 6. Experimental (■) and calculated (—) resonance Raman excitation profile of the six most intense vibrational modes of alizarin adsorbed on TiO_2 nanoparticles in aqueous solution at *p*H 3.

absorption spectra of free alizarin in solution is significantl different from that of the Alz|TiO_2 complex, consistent with strong adsorption, or chemisorption. This conclusion is consistent with the observed absorption spectra of chelated alizarin[53,54] which show dramatic absorption band shifts to the red upon chelation of the two hydroxy groups. However, the results reported here are different than previous resonance Raman spectra of adsorbates on TiO_2 surfaces.[36,39] For example, the resonance Raman and absorption spectra of adsorbed ruthenium complexes on TiO_2 surfaces are almost identical to those of the complexes in solution.[36,39] Also, early resonance Raman studies of adsorption of ruthenium complexes on TiO_2 surfaces showed intense low frequency TiO_2 vibrations with excitation within an adsorbate absorption band,[38,39] whereas later studies on related systems showed no such intense, low frequency modes.[37,40] These different results could be due to either mode-specifi dephasing of the adsorbate and/or TiO_2 vibrations (*vide infra*) or similar intensities of the Raman scattering from TiO_2 and the resonance Raman scattering of the complex. The lack of an excitation-wavelength dependence study of the resonance Raman spectra in the early studies suggested that the latter explanation is plausible. However, the extinction coefficient of one of the ruthenium complex dyes (8800 $cm^{-1}\,M^{-1}$) used previously and of alizarin (8700 $cm^{-1}\,M^{-1}$) used here are similar, suggesting the Raman intensities of TiO_2 relative to the resonance Raman intensities of the adsorbed dye should be similar in the two experiments.

An advantage of vibrational spectroscopy is that a more detailed picture of the chelating interaction can be obtained. The carbonyl stretching vibration at 1655 and 1690 cm^{-1} in uncomplexed alizarin is downshifted in the Alz|TiO_2 complex to overlapping bands centered at 1630 cm^{-1}. It has been suggested that the carbonyl and hydroxyl groups of alizarin could coordinate to a surface Ti^{4+} ion, forming a six-membered ring.[52] In this model, binding of the carbonyl would reduce the CO bond order and account for the observed downshift of the carbonyl vibration. An alternative model suggests that alizarin adsorbs via chelation of the two alizarin OH groups to a surface Ti^{4+} ion. This second model is supported by the observation that adsorption of alizarin follows a Langmuir-type isotherm with a stability constant identical to catechol adsorption.[25] The increased Raman intensity in the 1326 cm^{-1} C–O stretch also supports the idea that the hydroxy groups provide the primary bridging bonds and are strongly coupled to the interfacial charge transfer. In addition, several overlapping bands in the 1268–1326 cm^{-1} region have intensity derived from C–O and ring stretching modes. All these bands account for ~33% of the internal reorganization energy. Complexation of the hydroxy groups would also result in a downshift of the carbonyl vibrational frequency by inductively decreasing the bond order. Finally, these results are in agreement with other studies which show resonance enhancement of donor–acceptor bridging modes in charge transfer complexes. For example, the intermolecular stretch of the hexamethylbenzene–tetracyanoethylene charge transfer complex[55] and the bridging CN stretches[40,56,57] in $Fe(CN)_6^{4+}$-sensitized TiO_2 account for 11% and 44%, respectively, of the total internal reorganization energy.

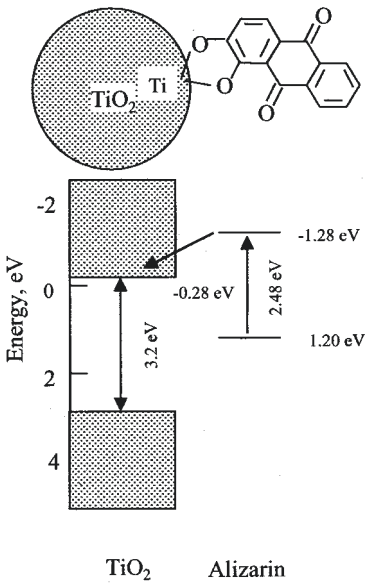

FIG. 7. Potential energy diagram of alizarin-sensitized TiO_2 nanoparticles. Alizarin oxidation potential (vs NHE) and conduction band edge of TiO_2 nanoparticle were from literature values (Refs. 25 and 52).

B. Charge transfer

Electron transfer (Fig. 7) from the firs excited singlet state of alizarin ($E_{00}=20\,010$ cm^{-1}, $E^0_{Alz+/Alz}=1.20$ V vs NHE) (Ref. 52) to the conduction band of a TiO_2 nanoparticle ($E_{\text{conduction band}}=-0.277$ V vs NHE) (Ref. 25) in aqueous solution at *p*H 3 is a highly exoergic reaction ($\Delta G=-1.0$ V). The resonance Raman spectrum presented here provides a detailed picture of the charge transfer event. Intense peaks in the 1200–1500 cm^{-1} region suggest that the charge transfer results in significan geometry changes along C═C, C–O–R, and ring vibrational modes, consistent with electron donation from alizarin to the conduction band of TiO_2 nanoparticles. The most intense bands in the resonance Raman spectrum of the Alz|TiO_2 complex are the C═C ring stretch at 1451 and 1461 cm^{-1}. These frequencies are close to the average quantized vibrational mode (~1500 cm^{-1}) assumed in modeling the quantum mechanical nature of molecules in electron transfer.[27,58] Evidently, this is a rough approximation of the true picture as these modes accounts for only ~36% of the internal barrier to electron transfer and are distributed over 20 vibrational modes coupled to electron transfer in this system, not one mode.

Surprisingly, no resonance enhancement is seen in the TiO_2 vibrational modes, most of which occur below 600 cm^{-1}. With this spectrometer, modes with significan intensity above 200 cm^{-1} should be readily observable. Thus, there appears to be no contribution to the internal reorganization energy from the TiO_2 acceptor. In contrast, the resonance Raman-derived internal reorganization energy is distributed roughly equally between donors and acceptors in charge transfer complexes composed of molecular species.[55,59,60] For example, in the hexamethylbenzene–

tetracyanoethylene charge transfer complex,[55] the donor and the acceptor account for 42% and 46% of the total internal reorganization energy of 0.26 eV, respectively. Similarly, in $Fe(CN)_6^{4-}|TiO_2$, in which the interaction is a weaker electrostatic physisorption, TiO_2 modes account for ~16% of the total reorganization energy.[57] The molecular mechanism behind this discrepancy is unclear. This discrepancy may arise from the small number of TiO_2 bonds involved in the charge transfer relative to the total number of TiO_2 bonds in the nanoparticle. Assuming a spherical TiO_2 nanoparticle with a diameter of 16 nm, there are on average $6-7\times10^4$ TiO_2 units per nanoparticle, of which roughly 9×10^3 will be distributed at the surface. Thus, at most only 15% of the TiO_2 units can possibly be involved in charge transfer with the adsorbed dye if alizarin is adsorbed to every TiO_2 unit at the surface. If the injected electron is rapidly delocalized over the entire nanoparticle, the change in any one TiO_2 may be very tiny, leading to very small geometry changes in the charge transfer excited state along TiO_2 vibrational coordinates. This rapid, mode-specific vibrational dephasing of the excited-state wave packet over the TiO_2 bath states would be expected to mode-specificall damp out the resonance Raman scattering from modes in the TiO_2 nanoparticle. The larger resonance Raman cross sections of the $Alz|TiO_2$ complex compared to free Alz in solution, with no consequent increase in TiO_2 vibrational intensities would be consistent with this model of the dephasing.

Alternatively, rapid electronic dephasing due to the high density of electronic states on the TiO_2 nanoparticle could damp out both the TiO_2 and the alizarin modes, if the coupling is strong enough. The anomalously low internal reorganization energy, compared to other charge transfer complexes, would be consistent with this mechanism of dephasing. In this model, then, the TiO_2 contribution to the reorganization energy would not show up in the mode-specifi contribution to the reorganization energy, but may be present in the dephasing, or outer-sphere, contribution to the reorganization energy. It must be emphasized that the terms ''inner-sphere'' and ''outer-sphere'' may not be as meaningful here as they are in homogeneous electron transfer. The total reorganization energy can be found from the Stokes shifts of the fluorescenc spectrum. Unfortunately, the $Alz|TiO_2$ complex is nonfluorescen due to rapid quenching by electron transfer. However, chemisorption of alizarin on ZrO_2 nanoparticles preserves many of the perturbations in electronic and nuclear structure, but the kinetics of electron transfer are much slower and fluorescenc is observed.[41] Using the fluorescenc Stokes shift for alizarin on ZrO_2 yields a total reorganization energy of 0.32 eV for the $Alz|TiO_2$ complex. Of this total, alizarin contributes 0.04 eV, the smallest internal reorganization energy reported so far for a macromolecular system and comparable to that of C_{60} (0.06 eV),[61] leaving 0.28 eV from the environment, i.e., solvent+TiO_2.

The environmental contribution to the reorganization energy can be calculated from the large Gaussian homogeneous broadening found in this study. Mukamel[62] has shown that the homogeneous broadening, $G(t)$ in Eqs. (3) and (4), can be related to the strength of coupling between the solvent and charge transfer complex within a Brownian oscillator model,

$$G(t)=\exp\{g_R(t)+ig_I(t)\}, \tag{5}$$

$$g_R(t)=(D^2/\Lambda^2)[\exp\{-\Lambda t/\hbar\}-1-\Lambda t/\hbar], \tag{6}$$

$$g_I(t)=(D^2/2kT\Lambda^2)[1-\exp\{-\Lambda t/\hbar\}], \tag{7}$$

where D is the coupling strength between the electronic transition and the solvent coordinates, and $\hbar/\Lambda$ is the characteristic time of the solvent modulation. The solvent reorganization energy (λ_s) in the static limit ($\Lambda \ll D$) is then just $D^2/2kT$. Fitting the phenomological Gaussian homogeneous linewidth used here in Eqs. (3) and (4) to Eqs. (5)–(7), yields values of $D=810$ cm^{-1}, $\Lambda=0.8$ cm^{-1}, and $\lambda_s=1630$ cm^{-1} (0.20 eV). The total reorganization energy of 0.24 eV is close to, but somewhat smaller than, the value obtained from the Stokes shift of the fluorescenc spectrum. This large reorganization energy and dephasing from the environment, which includes both the solvent and nanoparticle interior, is consistent with both the observed Stokes shift of 2800 cm^{-1} and the observed rapid cooling/relaxation in the TiO_2 nanoparticle.[41] The spectroscopic properties of alizarin-sensitized TiO_2 are insensitive to the nature of the solvent,[41] suggesting that the solvent itself plays a very minor role and that the majority of the dephasing contribution arises from the TiO_2 nanoparticle interior. Such a bath of vibrational states in the nanoparticle, coupled to the TiO_2 vibrations localized at the adsorption site may rapidly dephase and severely damp the Raman scattering from the local TiO_2 vibrations, as well as those of the adsorbed dye.

Analysis of the absorption spectrum and resonance Raman excitation profile also requires incorporation of a large inhomogeneous broadening of 0.2 eV (Table I). The large inhomogeneous broadening in the $Alz|TiO_2$ complex may arise from a distribution of adsorption sites on the surface of TiO_2 nanoparticle. Each site may have different binding energy, orientation and solvation and, hence, a different electronic transition energy. These different sites may be the source for the multicomponent electron transfer rates observed in the $Alz|TiO_2$ complex.[41]

C. Implications to photovoltaic application

One of the most important criteria for achieving efficien photon to electrical energy conversion in a macromolecular assembly designed to mimic natural photosynthesis is to have a system with minimum reorganization energy to allow efficien charge separation.[63] This important criterion is fully exploited by nature in the primary electron transfer processes in photosynthesis. The chromophores (porphyrin–pheophytin–quinones) of the bacterial photosynthetic reaction center[63] are arranged in the protein matrix in such a way that it allows the system to have an extremely small reorganization energy ($\lambda_T=0.2$ eV). This allows ultrafast charge separation and retards the energy-wasting back electron transfer rate.

The $Alz|TiO_2$ system meets this basic criterion for effi cient electron transfer by having a small reorganization energy of only 0.24 eV. Gratzel *et al.* have shown that the

forward electron transfer rate in the Alz|TiO_2 complex is indeed very fast ($\tau < 100$ fs).[41] However, the back electron transfer rate is also very fast ($\tau \sim 450$ fs), in spite of the fact that the back electron transfer in Alz|TiO_2 system lies deep in the Marcus inverted region ($-\Delta G^0 = 1.48$ eV, and $\lambda_T = 0.25$ eV). It is possible that the large electronic coupling (0.38 eV) of this system and/or quantum effects play a decisive role in governing the rates of electron transfer.

Lastly, it is interesting to note that the reorganization energy of the Alz|TiO_2 complex is much smaller than many macromolecular systems designed to mimic photosynthesis, for example, porphyrin linked quinone (0.5–1.8 eV) (Refs. 64–66) and bisporphyrin linked system (0.5–1.5 eV).[67,68] This is one of the prime reasons for the success of dye sensitized TiO_2 for solar to electrical energy conversion.

VI. CONCLUSIONS

Quantitative resonance Raman intensity analysis of alizarin adsorbed on TiO_2 nanoparticles demonstrates that the alizarin is chemisorbed via chelation of the 1,2-hydroxy groups by a surface Ti^{4+} ion. Reorganization of the alizarin donor upon photoinduced electron injection dominates the resonance Raman spectrum with excitation in the 488 nm charge transfer transition, while TiO_2 reorganization appears to dominate the dephasing component of the homogeneous line shape necessary to reproduce the experimental resonance Raman excitation profile and absorption spectrum. The relatively small alizarin reorganization energy of 0.04 eV, compared to the total reorganization energy of 0.32 eV derived from the fluorescenc Stokes shift, suggests that the main reorganization occurs within the TiO_2 nanoparticle. Strong coupling of the TiO_2 interior to surface TiO_2 units involved in the primary charge transfer appear to damp out the Raman intensity of the TiO_2 vibrations, and perhaps the resonance Raman intensities of the adsorbed alizarin, via a mode-specifi dephasing mechanism, consistent with the ultrafast cooling/relaxation events seen in a previous study. The results show that resonance Raman spectroscopy can provide a sensitive partitioning of the reorganization energy among the different components of heterogeneous electron transfer systems. The study also highlights the need for further investigations into the interplay of electronic coupling, reorganization energy and quantum effects in the electron transfer rate in the Marcus inverted region.

ACKNOWLEDGMENTS

The authors thank Professor J. Haber for useful discussions and NSERC Research Grants-in-Aid for providing funding for this work.

[1] R. J. D. Miller, G. L. McLendon, A. J. Nozik, W. Schmichler, and F. Willig, *Surface Electron-Transfer Processes* (VCH, New York, 1995).
[2] A. J. Nozik and R. Memming, J. Phys. Chem. **100**, 13061 (1996).
[3] P. V. Kamat, Prog. React. Kinet. **19**, 277 (1994).
[4] A. Hagfeldt and M. Gratzel, Chem. Rev. **95**, 49 (1995).
[5] P. V. Kamat and D. Meisel, *Semiconductor Nanoclusters Physical, Chemical, and Catalytic Aspects* (Elsevier, Amsterdam, 1997), Vol. 103.
[6] K. I. Jacobson and R. E. Jacobson, *Imaging Systems* (Wiley, New York, 1976).
[7] A. Hagfeldt and M. Gratzel, Acc. Chem. Res. **33**, 269 (2000).
[8] A. Kay and M. Gratzel, Sol. Energy Mater. Sol. Cells **44**, 99 (1996).
[9] B. O'Regan and M. Gratzel, Nature (London) **353**, 737 (1991).
[10] M. K. Nazeeruddin, P. Pechy, T. Renouard *et al.*, J. Am. Chem. Soc. **123**, 1613 (2001).
[11] R. Eichberger and F. Willig, Chem. Phys. **141**, 159 (1990).
[12] T. A. Heimer, E. J. Heilweil, C. A. Bignozzi, and G. J. Meyer, J. Phys. Chem. A **104**, 4256 (2000).
[13] J. M. Lanzafame, S. Palese, D. Wang, R. J. D. Miller, and A. A. Muenter, J. Phys. Chem. **98**, 11020 (1994).
[14] J. B. Asbury, E. Hao, Y. Wang, H. N. Ghosh, and T. Lian, J. Phys. Chem. B **105**, 4545 (2001).
[15] Y. Tachibana, S. A. Haque, I. P. Mercer, J. R. Durrant, and D. R. Klug, J. Phys. Chem. B **104**, 1198 (2000).
[16] G. Benko, M. Hilgendorff, A. P. Yartsev, and V. Sundstrom, J. Phys. Chem. B **105**, 967 (2001).
[17] J. Kallioinen, V. Lehtovuori, P. Myllyperkio, and J. Korppi-Tommola, Chem. Phys. Lett. **340**, 217 (2001).
[18] J. B. Asbury, R. J. Ellingson, H. N. Ghosh, S. Ferrere, A. J. Nozik, and T. Lian, J. Phys. Chem. B **103**, 3110 (1999).
[19] H. N. Ghosh, J. B. Asbury, and T. Lian, J. Phys. Chem. B **102**, 6482 (1998).
[20] A. Kay and M. Gratzel, J. Phys. Chem. **97**, 6272 (1993).
[21] J. He, A. Hagfeldt, S.-E. Lindquist, H. Grennberg, F. Korodi, L. C. Sun, and B. Akermark, Langmuir **17**, 2743 (2001).
[22] P. V. Kamat, S. Hotchandani, M. Delind, K. G. Thomas, S. Das, and M. V. George, J. Chem. Soc., Faraday Trans. **89**, 2397 (1993).
[23] I. Martini, J. H. Hodak, and G. V. Hartland, J. Phys. Chem. B **102**, 9508 (1998).
[24] S. Anderson, E. C. Constable, M. P. Dare-Edwards, J. B. Goodenough, A. Hamnett, K. R. Seddon, and R. D. Wright, Nature (London) **280**, 571 (1979).
[25] J. Moser, S. Punchihewa, P. P. Infelta, and M. Gratzel, Langmuir **7**, 3012 (1991).
[26] J. F. Smalley, S. W. Feldberg, C. E. D. Chidsey, M. R. Lindford, M. D. Newton, and Y. P. Liu, J. Phys. Chem. **99**, 13141 (1995).
[27] R. A. Marcus and N. Sutin, Biochim. Biophys. Acta **811**, 265 (1985).
[28] A. B. Myers, Chem. Rev. **96**, 911 (1996).
[29] J. L. McHale, Acc. Chem. Res. **34**, 265 (2001).
[30] A. B. Myers and R. A. Mathies, "Resonance Raman Intensities: A Probe of Excited-State Structure and Dynamics", in *Biological Applications of Raman Spectroscopy*, edited by T. G. Spiro (Wiley, New York, 1987), Vol. 2, p. 1.
[31] A. B. Myers, "Excited Electronic State Properties from Ground-State Resonance Raman Intensities, in *Laser Techniques in Chemistry*, edited by A. B. Myers and T. R. Rizzo (Wiley, New York, 1995), p. 325.
[32] A. M. Kelley, J. Phys. Chem. A **103**, 6891 (1999).
[33] J. F. Brazdil and E. B. Yeager, J. Phys. Chem. **85**, 995 (1981).
[34] J. F. Brazdil and E. B. Yeager, J. Phys. Chem. **85**, 1005 (1981).
[35] See EPAPS Document No. E-JCPSA6-116-703227 for Table II listing the experimental and calculated Raman cross sections for all of the vibrational modes as a function of excitation wavelength. This document may be retrieved via the EPAPS homepage (http://www.aip.org/pubservs/epaps.html) or from ftp.aip.org in the directory/epaps. See the EPAPS homepage for more information.
[36] W. Shi, S. Wolfgang, T. C. Strekas, and J. Gafney, J. Phys. Chem. **89**, 974 (1985).
[37] S. Umapathy, A. M. Cartner, A. W. Parker, and R. E. Hester, J. Phys. Chem. **94**, 8880 (1990).
[38] S. Umapathy, G. Lee-Son, and R. E. Hester, J. Mol. Struct. **194**, 107 (1989).
[39] S. Umapathy, G. Lee-Son, and R. E. Hester, J. Chem. Soc. Chem. Commun. 1841 (1987).
[40] R. L. Blackbourn, C. S. Johnson, and J. T. Hupp, J. Am. Chem. Soc. **113**, 1060 (1991).
[41] R. Huber, S. Sporlein, J. E. Moser, M. Gratzel, and J. Wachtveitl, J. Phys. Chem. B **104**, 8995 (2000).
[42] C. Kormann, D. W. Bahnemann, and M. R. Hoffmann, J. Phys. Chem. **92**, 5196 (1988).
[43] E. Fraga, A. Webb, and G. R. Loppnow, J. Phys. Chem. **100**, 3278 (1996).
[44] G. R. Loppnow and R. A. Mathies, Biophys. J. **54**, 35 (1988).
[45] K. K. Lehmann, J. Smolarek, O. S. Khalil, and L. Goodman, J. Phys. Chem. **83**, 1200 (1979).
[46] G. Smulevich, L. Angeloni, S. Giovannardi, and M. P. Marzocchi, Chem. Phys. **65**, 313 (1982).

[47] G. Smulevich and M. P. Marzocchi, Chem. Phys. **94**, 99 (1985).
[48] T. Sekiya, S. Ohta, S. Kamei, M. Hanakawa, and S. Kurita, J. Phys. Chem. Solids **62**, 717 (2001).
[49] T. Ohsaka, F. Izumi, and Y. Fujiki, J. Raman Spectrosc. **7**, 321 (1978).
[50] V. Peruzzo and R. E. Hester, J. Raman Spectrosc. **5**, 115 (1976).
[51] D. N. Adams, *Metal-Ligand and Related Vibrations* (Edward Arnold, London, 1967), p. 258.
[52] J. E. Moser and M. Gratzel, Chem. Phys. **176**, 493 (1993).
[53] M. Matsumura, Y. Nomura, and H. Tsubomura, Bull. Chem. Soc. Jpn. **49**, 1409 (1976).
[54] N. Dilawar and Z. H. Zaidi, Indian J. Chem. **30A**, 890 (1991).
[55] K. Kulinowski, I. R. Gould, N. S. Ferris, and A. B. Myers, J. Phys. Chem. **99**, 17715 (1995).
[56] S. K. Doorn, R. L. Blackbourn, C. S. Johnson, and J. T. Hupp, Electrochim. Acta **36**, 1775 (1991).
[57] J. T. Hupp and R. D. Williams, Acc. Chem. Res. **34**, 808 (2001).
[58] J. Jortner, J. Chem. Phys. **64**, 4860 (1976).
[59] D. Egolf, M. R. Waterland, and A. M. Kelley, J. Phys. Chem. B **104**, 10727 (2000).
[60] M. Lilichenko, D. Tittlebach-Helmrich, J. W. Verhoeven, I. R. Gould, and A. B. Myers, J. Chem. Phys. **109**, 10958 (1998).
[61] S. Larsson, A. Klimkans, L. Rodriguez-Monge, and G. J. Duskesas, J. Mol. Struct. **425**, 155 (1998).
[62] S. Mukamel, Annu. Rev. Phys. Chem. **41**, 647 (1990).
[63] C. C. Moser, J. M. Keske, K. Warncke, R. S. Farid, and P. L. Dutton, in *The Photosynthetic Reaction Center*, edited by J. Deisenhofer and J. R. Norris (Academic, San Diego, 1993), Vol. 2, Chap. 1, pp. 1–22.
[64] R. J. Harrison, B. Pearce, G. S. Beddard, A. J. Cowan, and J. K. M. Sanders, Chem. Phys. **116**, 427 (1987).
[65] T. Asahi, M. Ohkohchi, R. Matsusuka, N. Mataga, R. P. Zhang, A. Osuka, and K. Maruyamaa, J. Am. Chem. Soc. **115**, 5665 (1993).
[66] H. Tsue, H. Imahori, T. Kaneda, Y. Tanaka, T. Okada, K. Tamaki, and Y. Sakata, J. Am. Chem. Soc. **122**, 2279 (2000).
[67] A. Harriman, V. Heitz, and J.-P. Sauvage, J. Phys. Chem. **97**, 5940 (1993).
[68] A. Osuka, G. Noya, S. Taniguchi, T. Okada, Y. Nishimura, I. Yamazaki, and N. Mataga, Chem. Eur. J. **6**, 33 (2000).